

Supporting Online Information for

**Bio-inspired oxidation of methane in water catalyzed by N-bridged diiron
phthalocyanine complex**

Alexander B. Sorokin*, Evgeny V. Kudrik, Denis Bouchu

* To whom correspondence should be addressed.

E-mail: alexander.sorokin@ircelyon.univ-lyon1.fr

Materials and Methods

Kinetic analysis of methane oxidation

Supplementary Figs.S1 to S17

References

Materials

Solvents and chemicals were obtained from Sigma-Aldrich and used without purification unless indicated. Methane- ^{13}C , 99 atom % ^{13}C was purchased from Sigma-Aldrich. Labeled water H_2^{18}O (95.4 atom. % ^{18}O , 0.6 atom % ^{17}O , 4.0 atom % ^{16}O) was obtained from Euriso-top.

Synthesis of μ -nitrido-bis[tetra(tert-butyl)phthalocyaninatoiron] (FePc^tBu_4) $_2\text{N}$. Tetra-tert-butylphthalocyaninatoiron(II) was synthesised and purified as described previously [S1]. 0.4 g of FePc^tBu_4 and 2 g of NaN_3 were suspended in 70 ml of oxygen-free xylene under argon. The mixture was heated for 6 h at 150°C under intensive stirring. The reaction mixture was cooled and resulting dark blue solution was separated from undissolved material by filtration. The solution was chromatographed on Al_2O_3 (neutral) with CH_2Cl_2 to remove impurities. Then $(\text{FePc}^t\text{Bu}_4)_2\text{N}$ complex was collected using $\text{CH}_2\text{Cl}_2:\text{EtOH}$ (100:1) mixture as eluent. Evaporation of solvent afforded pure $(\text{FePc}^t\text{Bu}_4)_2\text{N}$ as a dark blue powder (yield 0.25 g, 62 %). ESI-MS: 1599.9 [M] $^+$ (100 %); calcd for $\text{C}_{96}\text{H}_{96}\text{N}_{17}\text{Fe}_2$: 1599.6. UV-Vis λ_{max} (log ϵ) (MeCN) : 219 (5.67); 272 (5.50); 340 (5.39); 637 (5.57). ^1H NMR (250 MHz, CDCl_3): 7.78 (s, 1H); 7.66 (s, 2H); 1.32 (s, 9 H). IR (KBr) 938 (ν_{as} Fe=N). ESR: Solid state or solution in acetone: singlet signal at $g = 1.99$.

μ -Oxo-bis[tetra(t-butyl)phthalocyaninatoiron(III)] and μ -carbido-bis[tetra(t-butyl)phthalocyaninatoiron(IV)] were prepared according to published methods [S2, S3].

Characterization of $(\text{FePc}^t\text{Bu}_4)_2\text{N}$. See Supplementary Figures S1 – S7.

Preparation of supported catalyst

28 mg of $(\text{FePc}^t\text{Bu}_4)_2\text{N}$ were dissolved in 50 ml of CH_2Cl_2 and 1 g of silica (Degussa Aerogel, specific surface - $200\text{ m}^2/\text{g}$) was added into solution. The resulting mixture was stirred for 2 h at room temperature and the solvent was evaporated under reduced pressure. The solid material was dried in vacuum at room temperature for 1 hour and at 50°C for 6 hours. The typical complex loadings were 17.5 – 18.5 $\mu\text{mol/g}$. DR UV-vis spectrum of supported catalyst exhibited absorption bands at 350, 457 nm and large absorption band at 636 nm (Supporting Figure S8).

Typical procedure for oxidation of methane

Methane oxidation was performed in a 37 mL cylindrical stainless steel autoclave with a teflon liner inside. The reactor was charged with 50 mg of $(\text{FePc}^t\text{Bu}_4)_2\text{N-SiO}_2$ containing 0.875-0.925 μmol of complex, 2 mL of water, 60 μL of 35 % hydrogen peroxide solution in water (678 μmol of oxidant) and 32 bars of methane. The reactor was heated at desired temperature (25-80°C) with magnetic stirring for 20 hours. Then the autoclave was cooled to 0°C and depressurised. The solid catalyst was separated by filtration using 0.45 μm filter and the liquid and gas phases were analysed by GC-MS.

Equipment and Methods

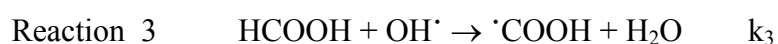
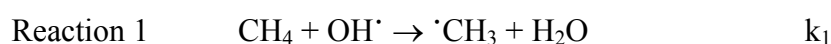
Liquid-state nuclear magnetic resonance spectra were obtained using a AM 250 Bruker spectrometer. The UV-vis spectra of solutions and the diffuse reflectance UV-vis spectra of solid catalysts were recorded on a Perkin-Elmer Lambda 35 spectrophotometer. The reaction products were identified and quantified by GC-MS method (Hewlett Packard 5973/6890 system ; electron impact ionization at 70 eV, He carrier gas, 30m x 0.25 mm HP-INNOWax capillary column, polyethylene glycol (0.25 μm coating). Infrared spectra were recorded on a Bruker Vector 22 FTIR spectrometer using KBr pellets. EPR spectra of solid $(\text{FePc}^t\text{Bu}_4)_2\text{N}$ were recorded on a Bruker Elexsys e500; conditions : 25°C, microwave frequency 9.415 GHz, power 0.4 mW, modulation 1.0 mT/100 kHz. EPR spectra of $(\text{FePc}^t\text{Bu}_4)_2\text{N}$ solution in acetone before and after addition of 5 equivs. of H_2O_2 were measured at a Bruker Elexsys e500 using capillary tube; conditions: 25°C, microwave frequency 9.392 GHz, power 40 mW, modulation 1.0 mT/100 kHz. X-ray photoelectron spectroscopy (XPS) spectra were collected with Kratos Axis Ultra DLD instrument using a hemispherical analyzer and working at a vacuum better than 10^{-9} mbar. All the data were acquired using monochromated Al K_α X-rays (1486.6 eV, 150 W), a pass energy 160 eV and 1 eV step size for wide scan and 40 eV pass energy with 0.1 eV step size for elemental scan, and a hybrid lens mode. The area analysed is 700 μm x 300 μm . Charge neutralisation was required for all samples. The peaks were referenced to the C-(C,H) components of the C1s band at 284.6 eV.

The yield of formic acid was determined by GC-MS using isobutyric acid as the external standard (Agilent 5973/6890 system; electron impact ionization at 70 eV, He carrier gas, 30 m x 0.25 mm HP-INNOWAX capillary column). The yield of formaldehyde was determined by Nash method [S4].

The labelling experiments were performed using approximately 1:1 mixture of $^{13}\text{CH}_4$ (99 atom % ^{13}C , Sigma-Aldrich) and CH_4 . The exact composition of this mixture was determined by mass spectrometry to be 53.0 % of CH_4 and 47.0 % of $^{13}\text{CH}_4$. Isotopic composition of formic acid was determined by GC-MS using m/z intensities. Each sample was analyzed three times and m/z intensities were obtained by an integration of all scans of the peak [S5]. In the absence of isotope labelling experiments published data on CH_4 oxidation in acetonitrile are not necessarily very reliable.

Kinetic analysis of methane oxidation : hypothesis of the involvement of OH \cdot radical

When the oxidation of methane is performed in MeCN, OH \cdot radical would react with CH_4 , CH_3CN and HCOOH according reactions 1-3 with reaction rates k_1 , k_2 and k_3 , respectively.



The literature values of these reaction constants are equal to (298 K, in $\text{cm}^3 \text{ molecule}^{-1} \text{ s}^{-1}$):

$$k_1 = 6.3 \times 10^{-15} \text{ [S6-S8]}$$

$$k_2 = 1.9 \times 10^{-14} \text{ [S9]}$$

$$k_3 = 4.5 \times 10^{-13} \text{ [S8]}$$

Solubility of methane in experimental conditions is about 0.02 M [S10]. Concentration of MeCN in pure MeCN is equal to 19.17 M.

If OH radical would be involved, the ratio

$$\underline{\text{Products derived from CH}_4} = \underline{6.3 \times 10^{-15} \times 0.02 \text{ M}} = 1:2890.$$

$$\text{Products derived from MeCN} \quad 1.9 \times 10^{-14} \times 19.17 \text{ M}$$

Isotope effect of the reaction of OH radical with C-H/C-D bonds is close to 1 and can not significantly change this ratio. This reactivity ratio $P_{\text{CH}_4} / P_{\text{MeCN}} = 1:2890$ is very different from the experimental ratio $P_{\text{CH}_4} / P_{\text{MeCN}} = 2:1$. Consequently, the possible involvement of OH radical in $(\text{FePc}^t\text{Bu}_4)_2\text{N} - \text{H}_2\text{O}_2$ system is not compatible with the experimental data and should be ruled out.

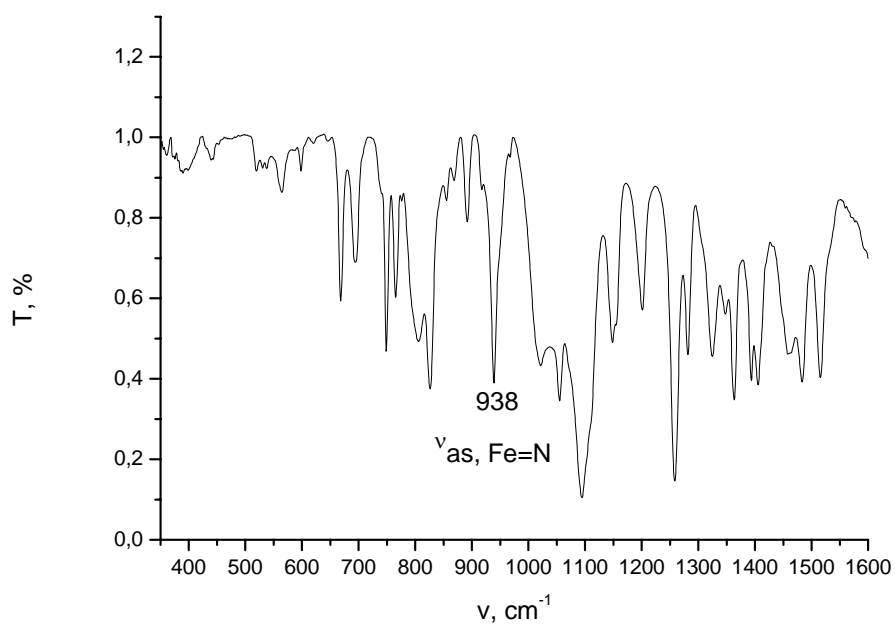
The same conclusion can be made from the estimation of maximal possible concentration of HCOOH. The concentration of methane, 0.02 M, is practically constant during experiment. In this case

$$[\text{HCOOH}]_{\text{max}} = k_1 [\text{CH}_4] / k_3 = 6.3 \times 10^{-15} \times 0.02 \text{ M} / 4.5 \times 10^{-13} = 0.00028 \text{ M}.$$

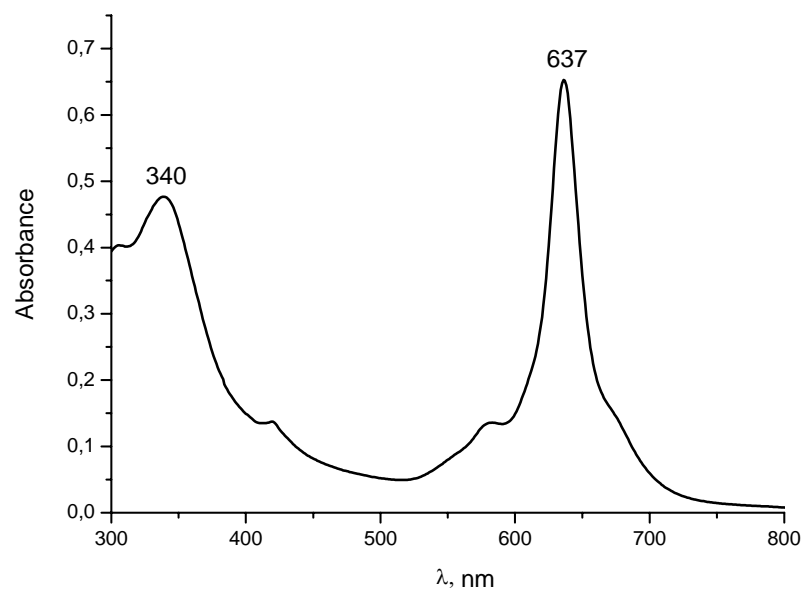
Thus, the maximal possible concentration of HCOOH in the case of free radical chemistry would be 0.00028 M. Experimentally obtained $[\text{HCOOH}]_{\text{water}} = 0.012 \text{ M}$ and $[\text{HCOOH}]_{0.1\text{M H}_2\text{SO}_4} = 0.069 \text{ M}$ are 43 and 246 times higher than maximal possible HCOOH concentration if free radical chemistry would be involved. Consequently, above kinetic analysis is not compatible with involvement of OH radical in $(\text{FePc}^t\text{Bu}_4)_2\text{N} - \text{H}_2\text{O}_2$ system.

References

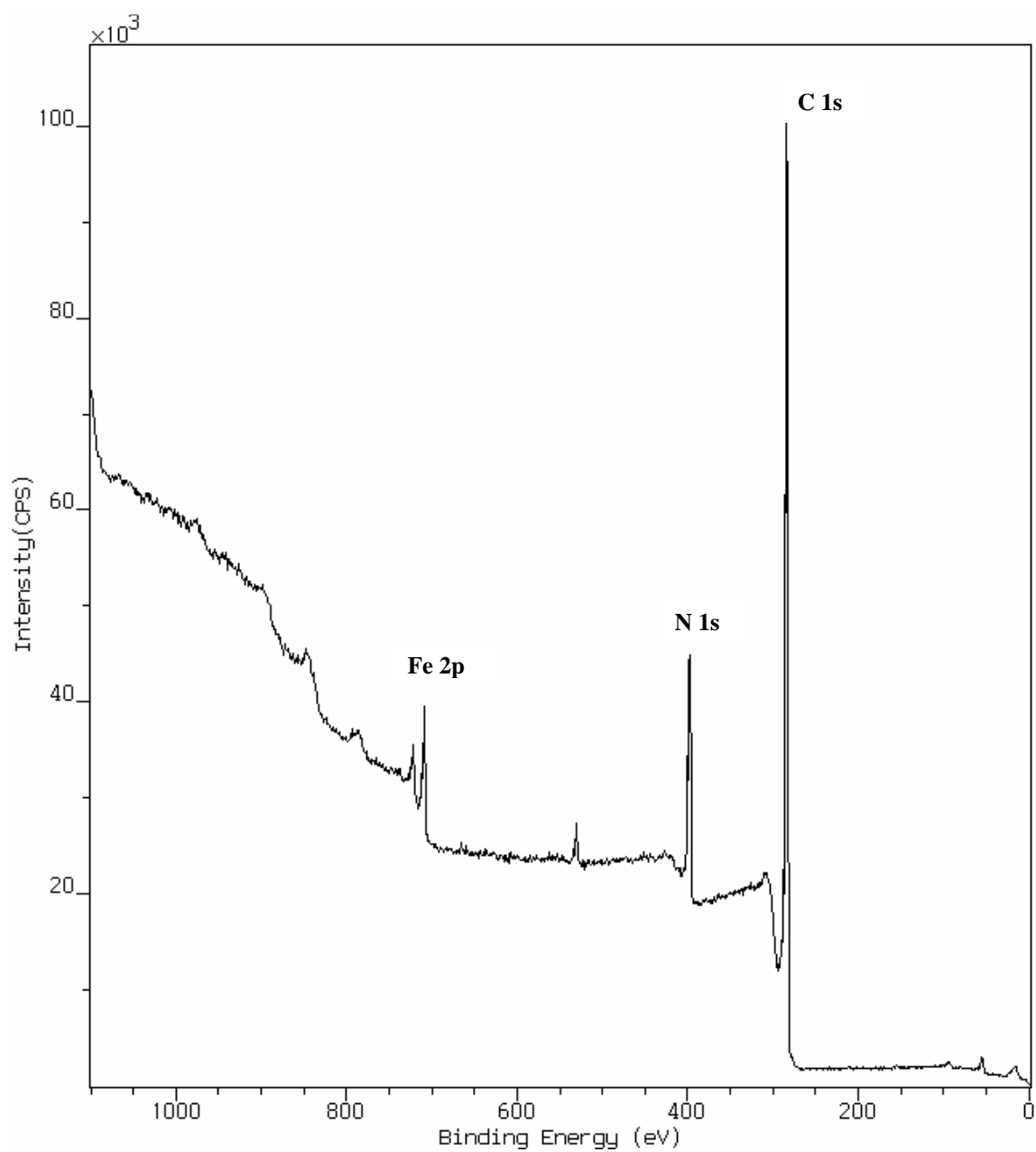
- S1. J. Metz, O. Schneider, M. Hanack, *Inorg. Chem.* 1984, **23**, 1065.
- S2. F. Monacelli, C. Ercolani, *C. Inorg. Chim. Acta* **2003**, 346, 95.
- S3. C. Ercolani, M. Gardini, V. L. Goedken, G. Pennesi, G. Rossi, U. Russo, P. Zanonato, *Inorg. Chem.* **1989**, 28, 3097.
- S4. G. L. Kedderis, D. R. Koop, P. F. Hollenberg, *J. Biol. Chem.* **1980**, 255, 10174.
- S5. A. B. Sorokin, A. Robert, B. Meunier, *J. Am. Chem. Soc.* **1993**, 115, 7293.
- S6. R. Atkinson, D.L. Baulch, R.A. Cox, R.F. Hampson, J.A. Kerr, M.J. Rossi, J. Troe, *J. Phys. Chem. Ref. Data* **1997**, 26, 521.
- S7. W.B. DeMore, S.P. Sandler, D.M. Golden, R.F. Hampson, M.J. Kurilo, S.J. Howard, A.R. Ravishankara, S.E. Kolb, M.J. Molina, *Chemical Kinetics and Photochemical Data for Use in Stratospheric Modeling: Evaluation Number 12*; Publication 97-4; National Aeronautic and Space Administration, Jet Propulsion Laboratory, California Institute of Technology: Pasadena, CA, 1997.
- S8. I.W.M. Smith, A.R. Ravishankara, *J. Phys. Chem.* **2002**, 106, 4798.
- S9. M.J. Kurylo, G.L. Knable, *J. Phys. Chem.* **1984**, 88, 3305.
- S10. Z. Duan, S. Mao, *Geochim. Cosmochim. Acta* **2006**, 70, 3369 and references therein.



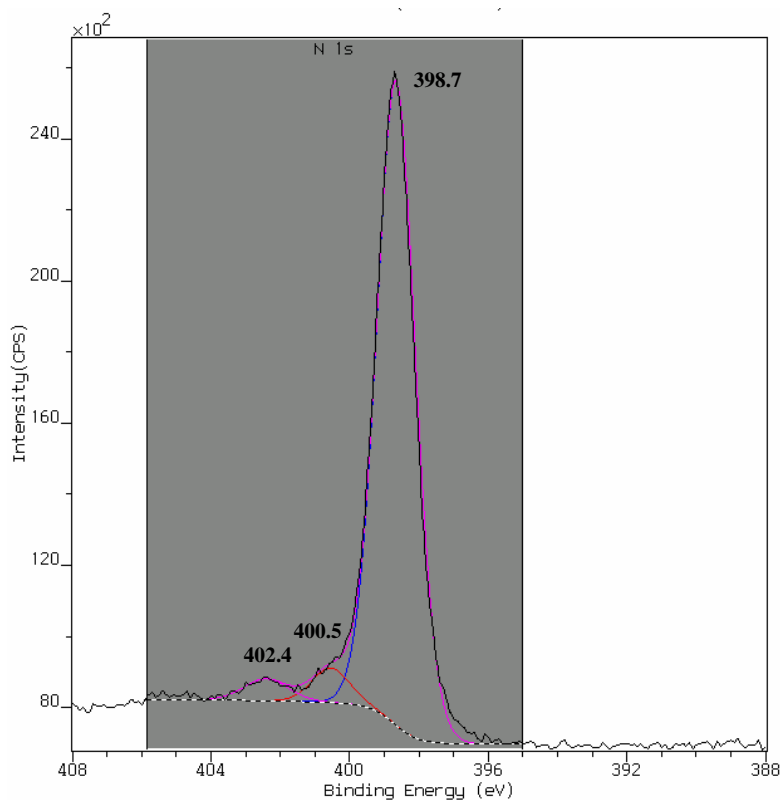
Supplementary Figure 1. IR spectrum of (FePc^tBu₄)₂N in KBr.



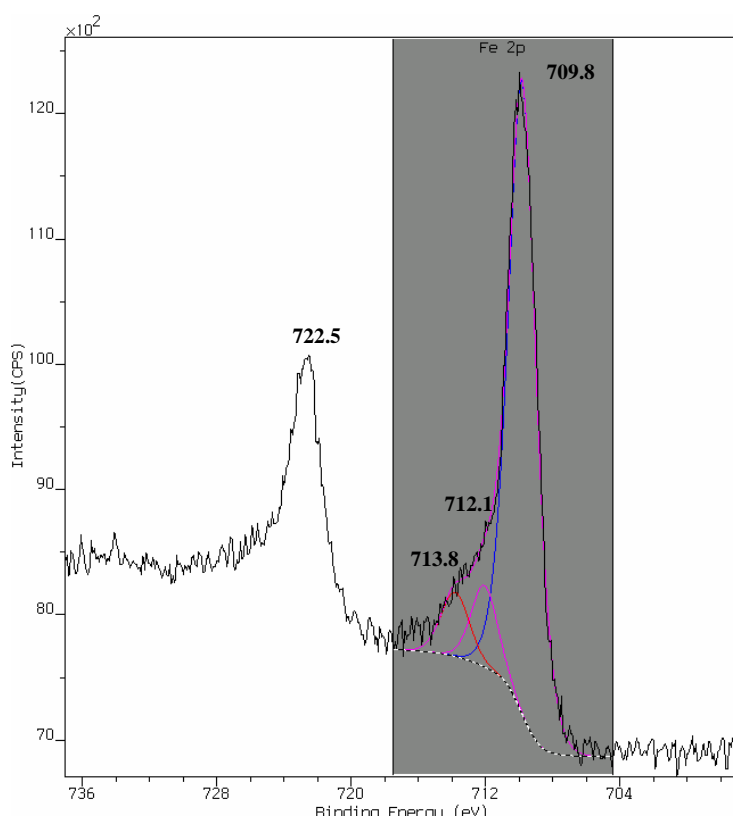
Supplementary Figure 2. UV-vis spectrum of (FePc^tBu₄)₂N in acetonitrile.



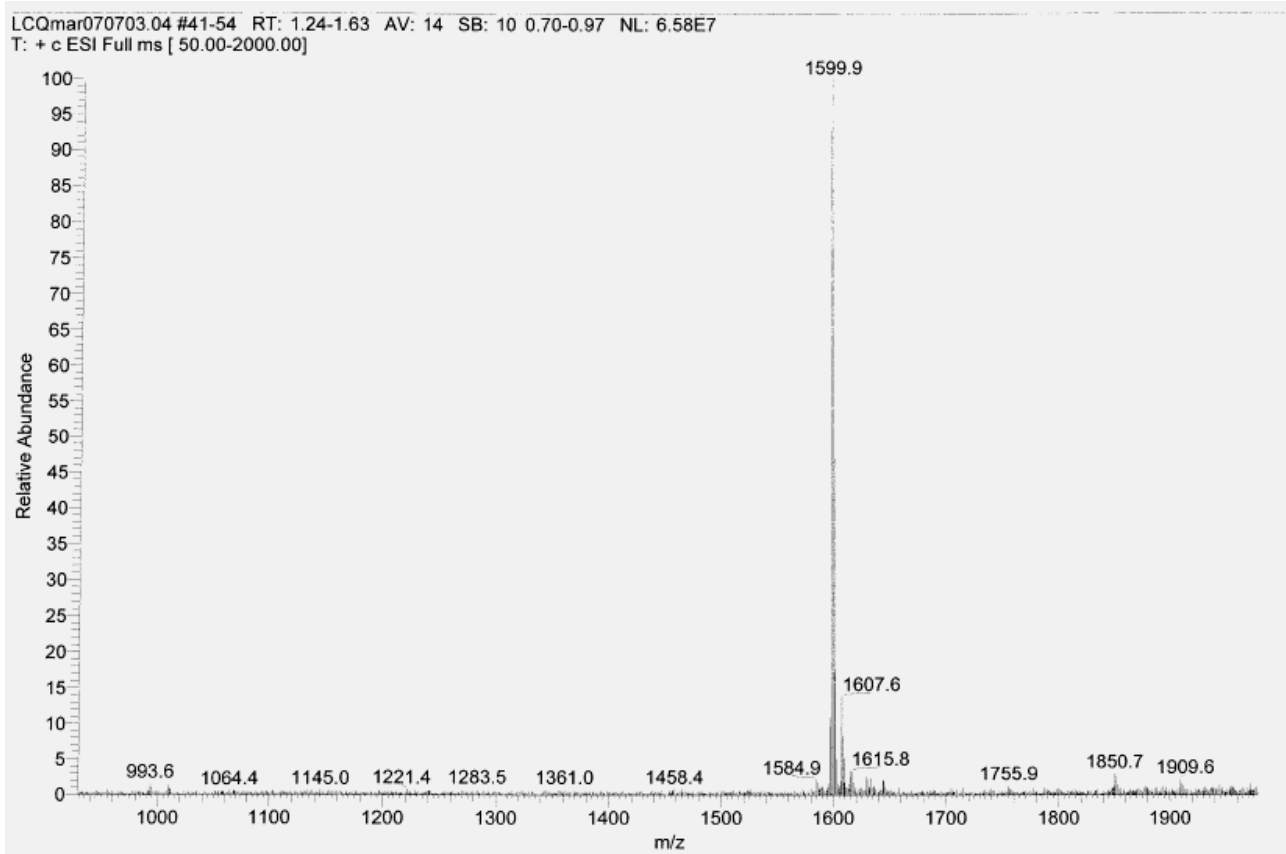
Supplementary Figure 3. XPS spectrum of $(\text{FePc}^t\text{Bu}_4)_2\text{N}$.



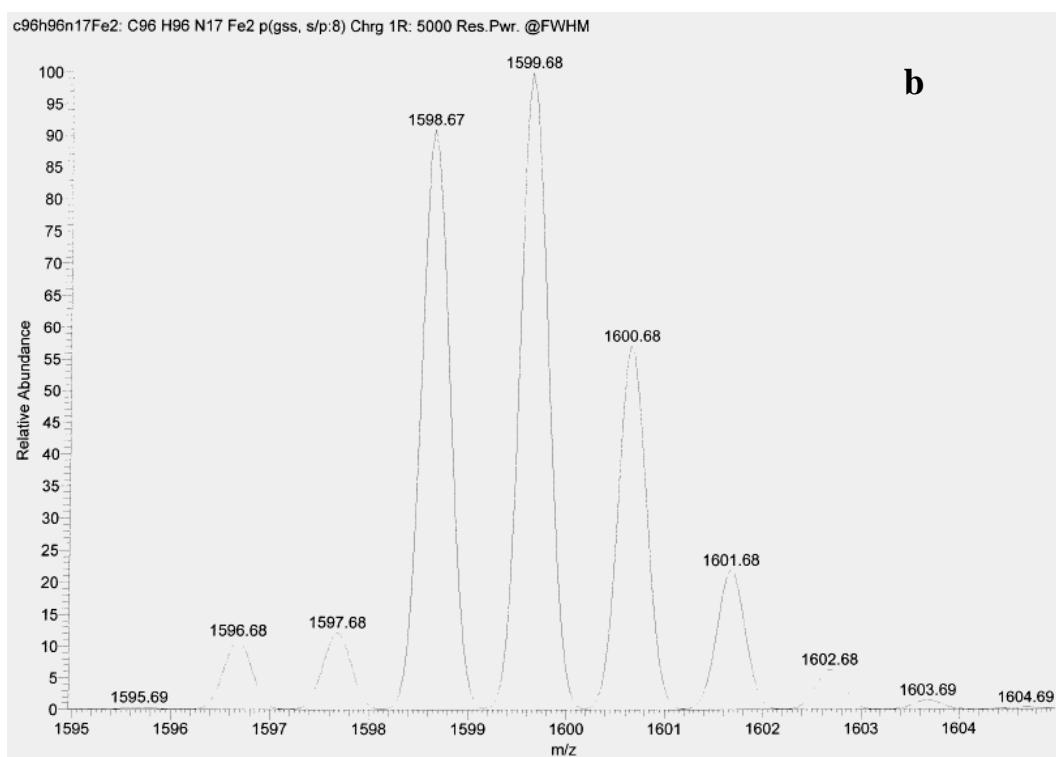
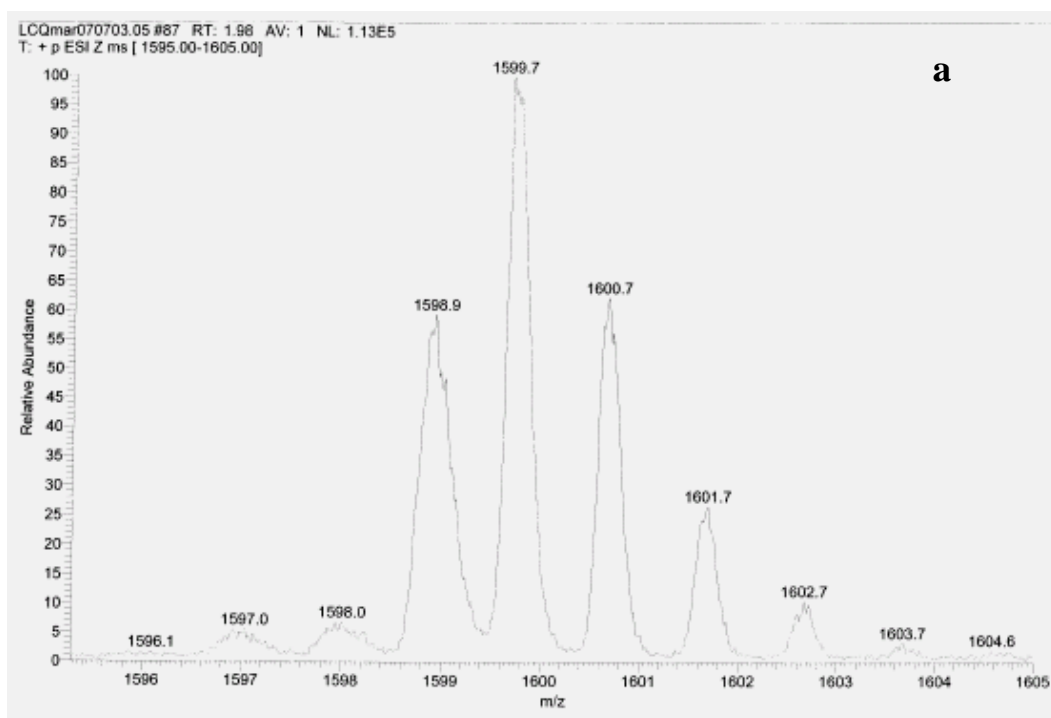
Supplementary Figure 4. Expansion of XPS spectrum (388-408 eV, N 1s) for (FePc^tBu₄)₂N. The 1s N XPS spectrum along with strong signal at 398.7 eV from nitrogen atoms of phthalocyanine cycle exhibits a small signal at 402.4 eV which can be assigned to strongly bonded bridging nitrogen.



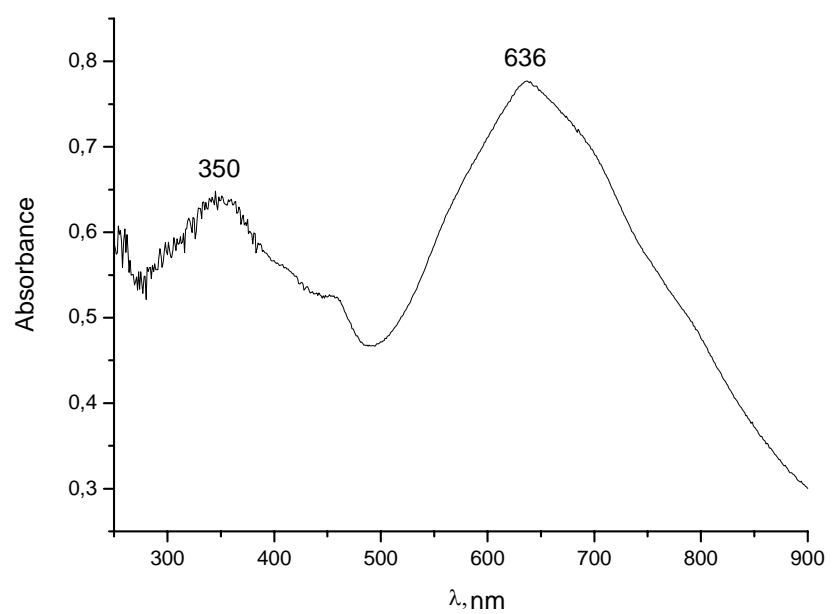
Supplementary Figure 5. Expansion of XPS spectrum (696-736 eV, Fe 2p) for (FePc^tBu₄)₂N.



Supplementary Figure 6. ESI-MS spectrum of $(\text{FePc}^t\text{Bu}_4)_2\text{N}$.

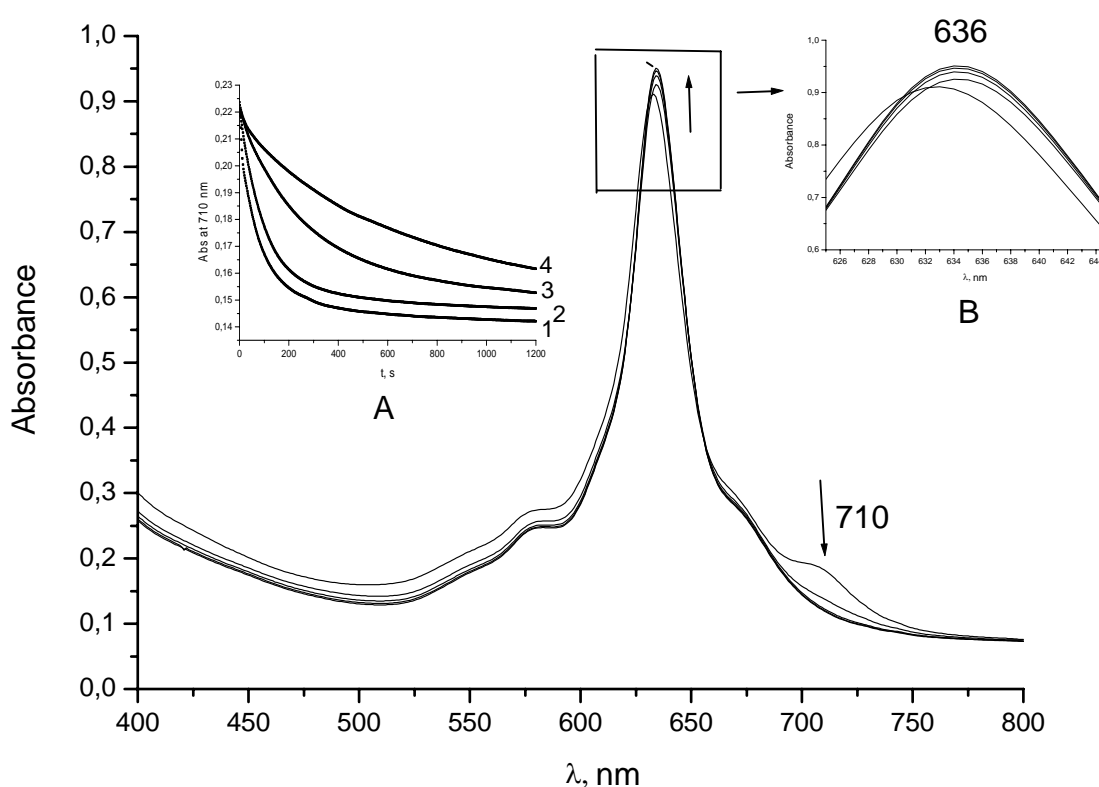


Supplementary Figure 7. Molecular peak cluster of $(\text{FePc}^t\text{Bu}_4)_2\text{N}$ in ESI-MS spectrum (a) and theoretical molecular peak cluster for $(\text{FePc}^t\text{Bu}_4)_2\text{N}$, $\text{C}_{96}\text{H}_{96}\text{N}_{17}\text{Fe}_2$ (b).

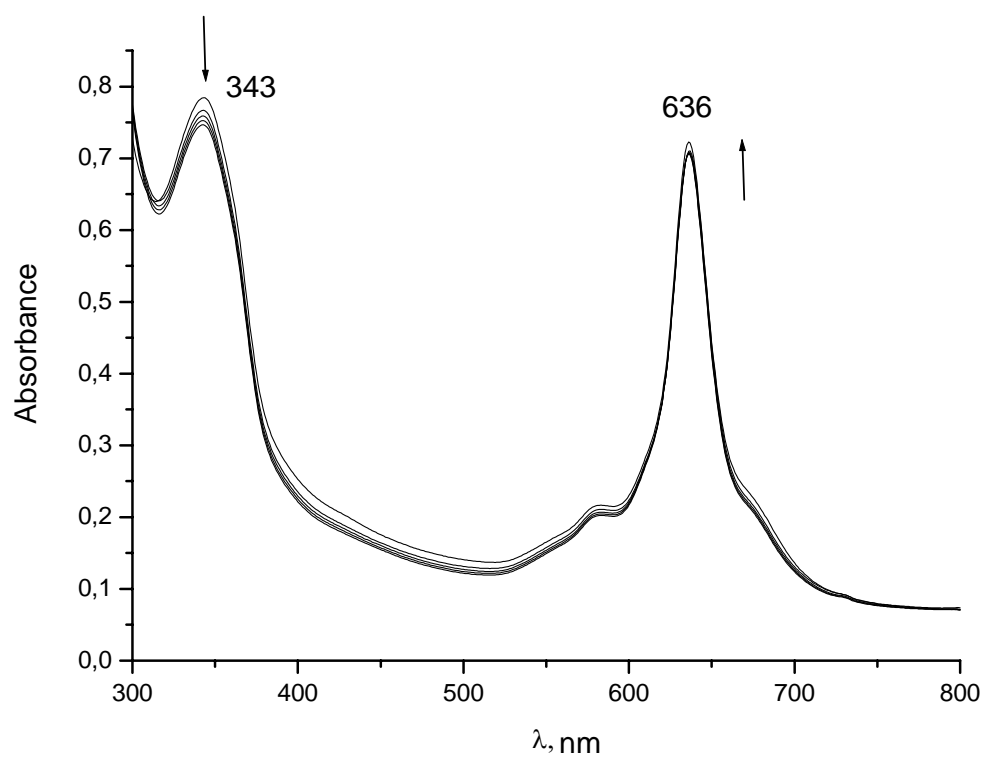


Supplementary Figure 8. Diffuse reflectance UV-vis spectrum of supported catalyst $(\text{FePc}^t\text{Bu}_4)_2\text{N-SiO}_2$.

Interaction of $(\text{FePc}^t\text{Bu}_4)_2\text{N}$ with hydrogen peroxide. Hydrogen peroxide (1000 fold excess) was added to the solution of $(\text{FePc}^t\text{Bu}_4)_2\text{N}$ in acetone or in MeCN in closed thermostated cuvette. The reaction was followed by UV-vis at $\lambda=636$ nm (Supplementary Fig. 9a and 9b). The changes of UV-vis spectra upon H_2O_2 addition were more pronounced in acetone. The intensity of Q band at 636 nm ($\pi - \pi^*$ phthalocyanine transition) was slightly increased and weak band at 710 nm disappeared. These changes indicate a metal-centered reaction with H_2O_2 without significant transformation of phthalocyanine macrocycle and monomerization. Monomeric phthalocyanine forms exhibit Q band in 665 – 680 nm region. The rate of the spectral changes correlates with H_2O_2 concentration (Inlet A). These observations indicate the interaction of H_2O_2 with diiron N-bridged phthalocyanine.

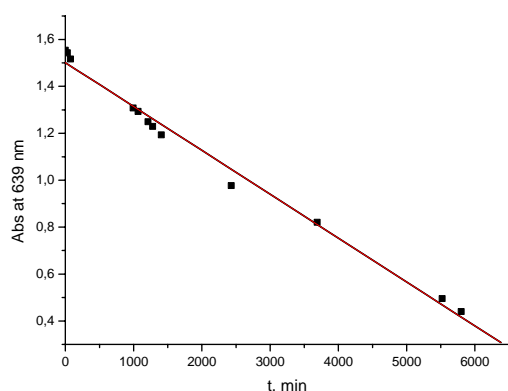


Supplementary Figure 9a. UV-Vis spectral changes during the reaction of $(\text{FePc}^t\text{Bu}_4)_2\text{N}$ with 1000 equivs of H_2O_2 . Conditions: a) acetone, 25°C , $[(\text{FePc}^t\text{Bu}_4)_2\text{N}] = 1.12 \times 10^{-5}$ M. Inlet A : kinetic curves of interaction of $[(\text{FePc}^t\text{Bu}_4)_2\text{N}$ with H_2O_2 ; $[\text{H}_2\text{O}_2] = 3.4 \times 10^{-3}$ M (curve 1), 2.26×10^{-3} (curve 2), 5.65×10^{-4} (curve 3), 2.82×10^{-4} (curve 4).



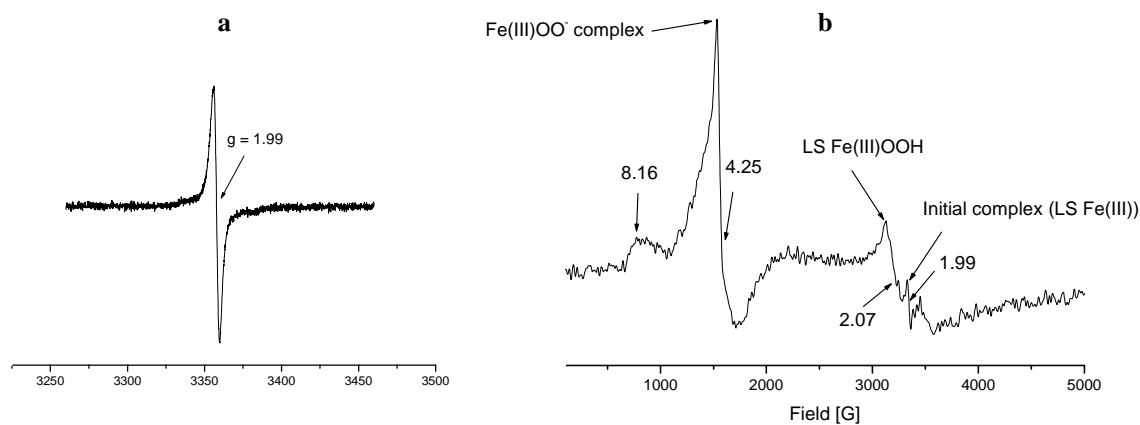
Supplementary Figure 9b. UV-Vis spectral changes during the reaction of $(\text{FePc}^t\text{Bu}_4)_2\text{N}$ with 1000 equivalents of H_2O_2 . Conditions: MeCN, 25°C , $[(\text{FePc}^t\text{Bu}_4)_2\text{N}] = 0.98 \times 10^{-5} \text{ M}$.

The life half-time ($\tau_{1/2}$) of μ -nitrido iron complex in the presence of H_2O_2 was determined from the decrease at $\lambda=639$ nm as indicated at Supplementary Fig. 10, where $\text{Abs} = A_t - A_\infty$. $\tau_{1/2} = 3470$ min at 25°C , $\tau_{1/2} = 560$ min at 60°C (not shown).



Supplementary Figure 10.

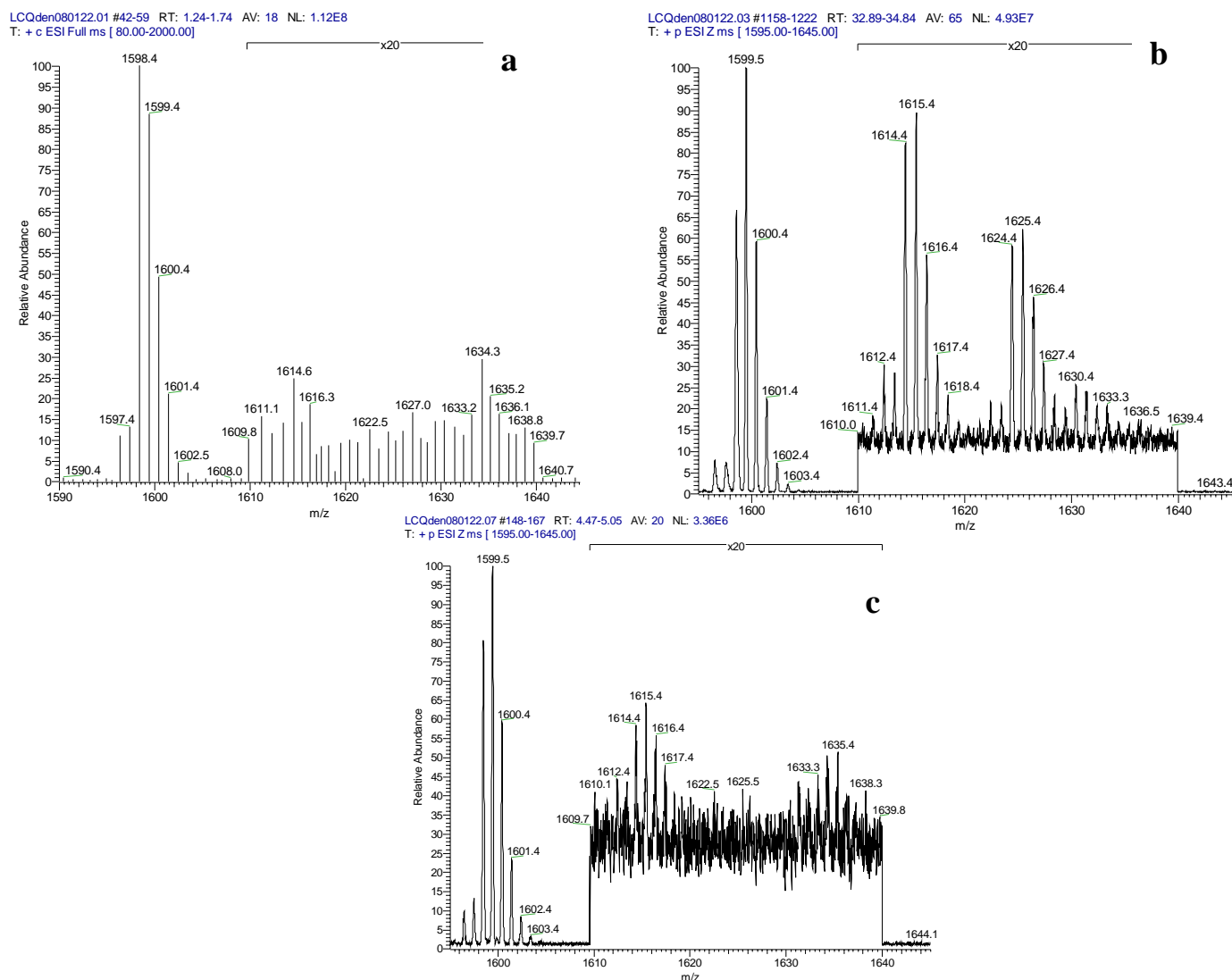
Degradation of μ -nitrido iron complex in the presence of 1000 equivs of H_2O_2 at 25°C .



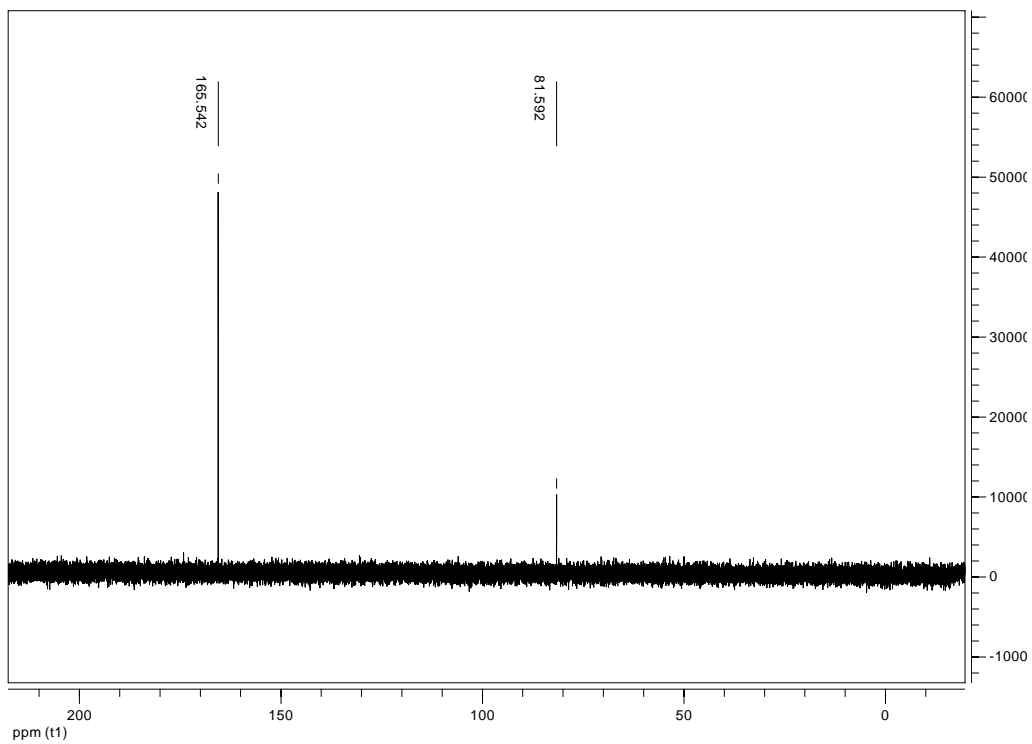
Supplementary Figure 11. EPR spectra of $(\text{FePc}^t\text{Bu}_4)_2\text{N}$ in acetone before (a) and after addition of 5 equivs of H_2O_2 (b). Conditions : capillary tube, 25°C , microwave frequency 9.392 GHz, power 40 mW, modulation 1.0 mT/100 kHz.

ESI-MS study of the interaction of H₂O₂ with (FePc^tBu₄)₂N. Evidence for oxo complex of (FePc^tBu₄)₂N.

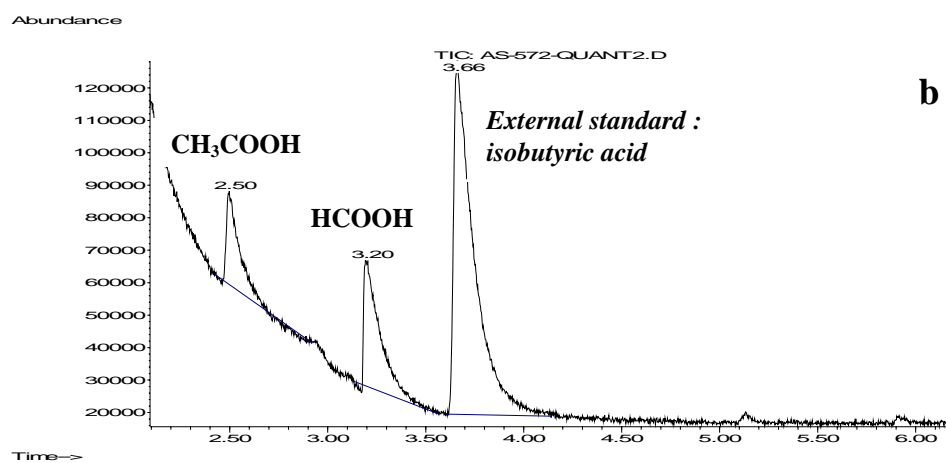
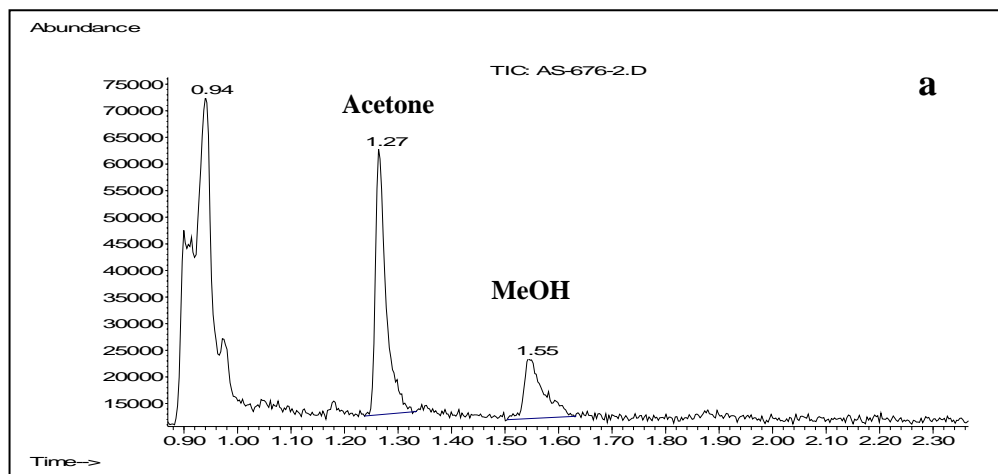
The solution of (FePc^tBu₄)₂N in MeCN (acetone is not a good solvent for ESI-MS method) exhibited a MS spectrum with molecular peak M⁺. When ~ 1000 fold excess of H₂O₂ was added, a (M + O)⁺ molecular cluster centered at m/z = 1615 was formed. During this experiment, after reaction time about 30 min., an additional species centered at m/z = 1625 was formed. This (M + CN)⁺ species can be derived from the oxidation of MeCN. This result is in accordance with our catalytic data. The formation of NCCN was observed by GC-MS. The (M + O)⁺ molecular cluster was almost disappeared upon addition of easily oxidizable cyclohexene. This observation strongly suggests that oxygen derived from H₂O₂ is bonded to iron center, not at phthalocyanine ring.



Supplementary Figure 12. ESI-MS spectra of **a**) solution of (FePc^tBu₄)₂N in MeCN; **b**) solution of (FePc^tBu₄)₂N in MeCN in the presence of H₂O₂ (after 33 min); **c**) the solution obtained after addition of cyclohexene to MeCN solution containing (FePc^tBu₄)₂N and H₂O₂. The spectrum **c**) was recorded 10 min after addition of cyclohexene. For all spectra 20-fold zoom was applied for 1610 – 1640 region.

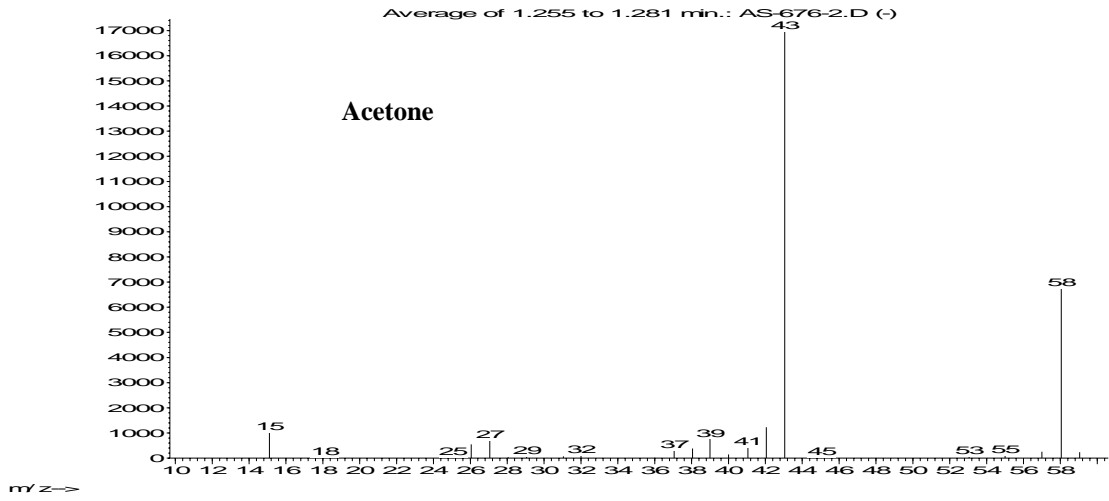


Supplementary Figure 13 ^{13}C NMR spectrum of the crude aqueous solution from the oxidation of the mixture of $^{13}\text{CH}_4$ and CH_4 in D_2O at 60°C .

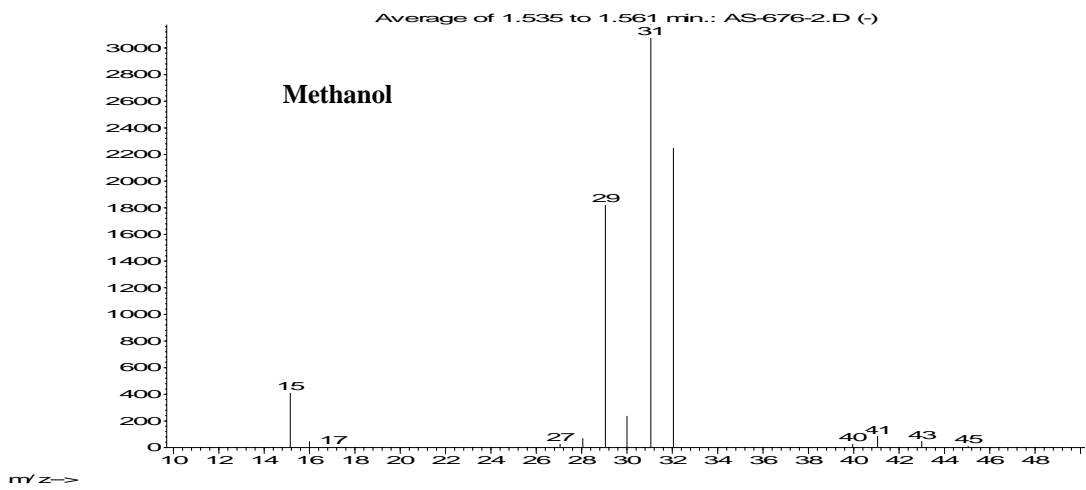


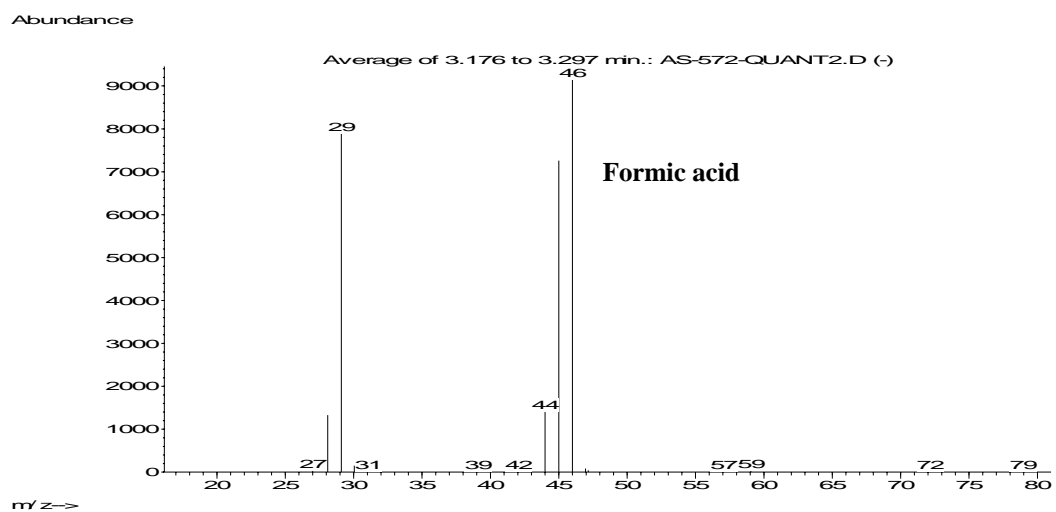
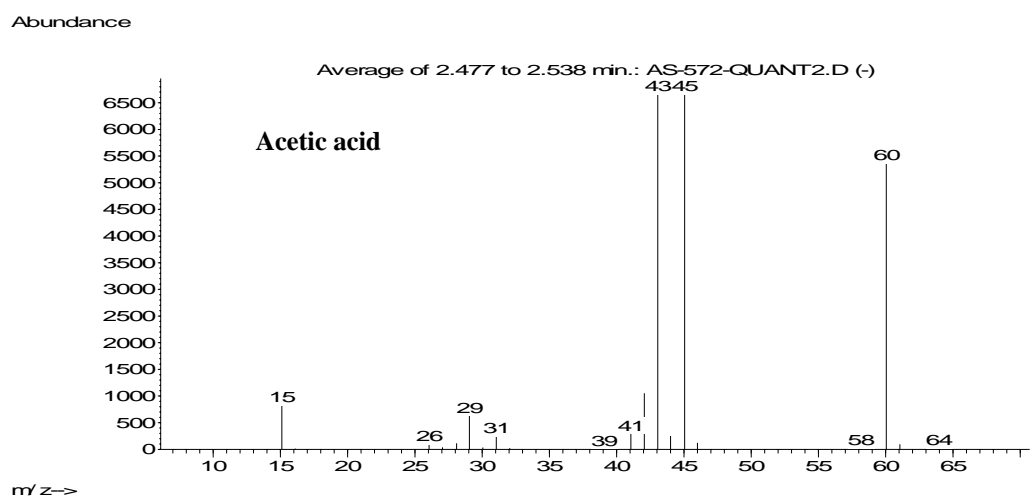
Supplementary Figure 14. Typical chromatograms of GC-MS analysis of aqueous reaction mixture after oxidation of methane : before water peak (a) and after water peak (b). Response factors of CH₃COOH and HCOOH with respect to isobutyric acid were 0.98 and 0.30, respectively.

Abundance

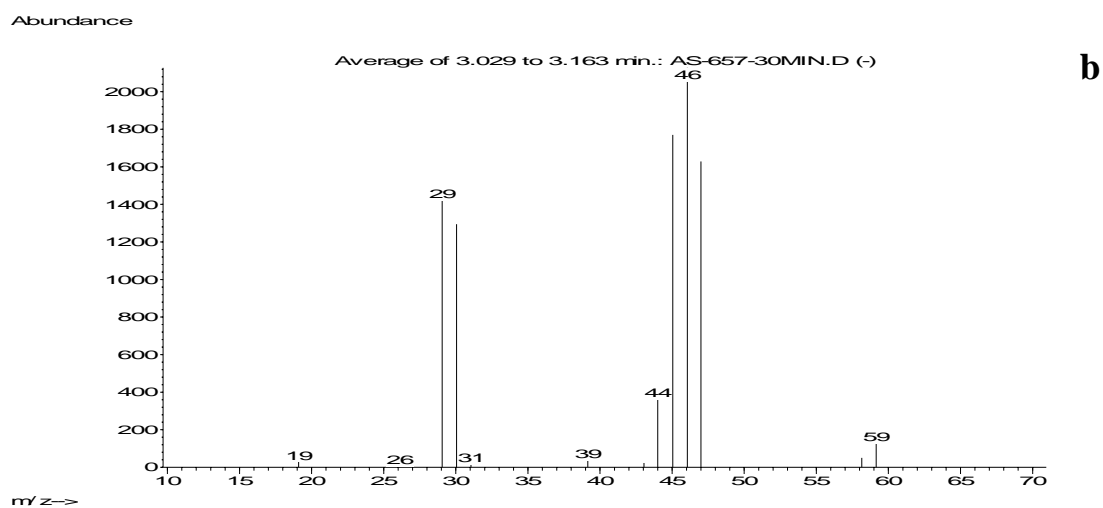
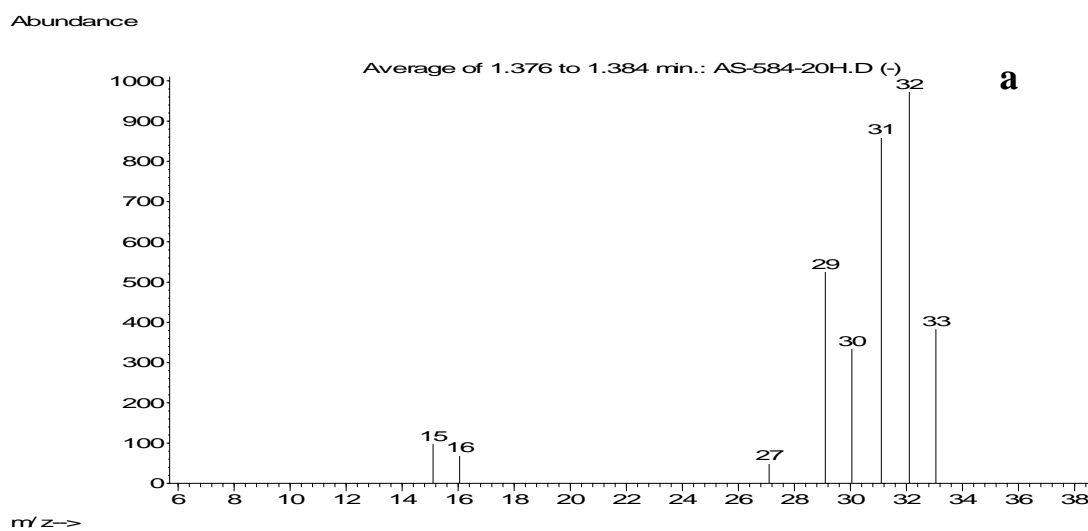


Abundance

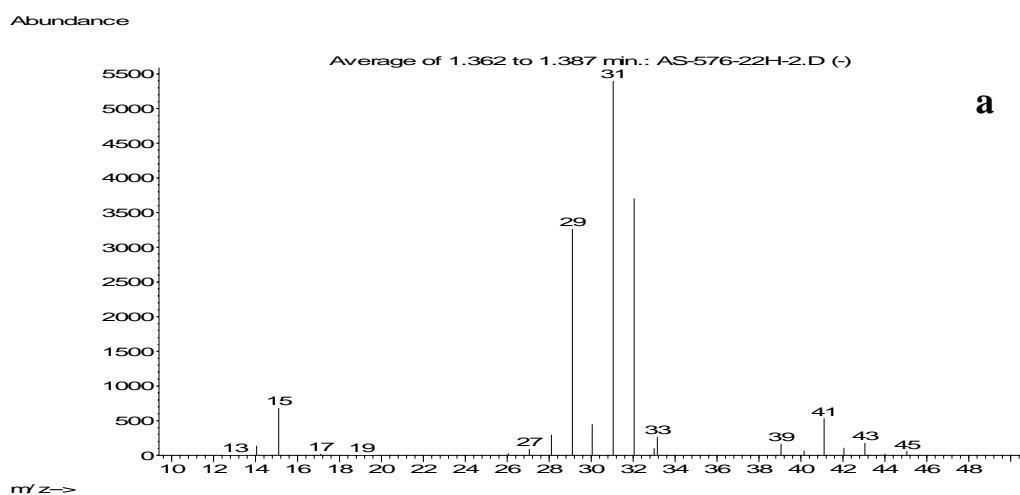




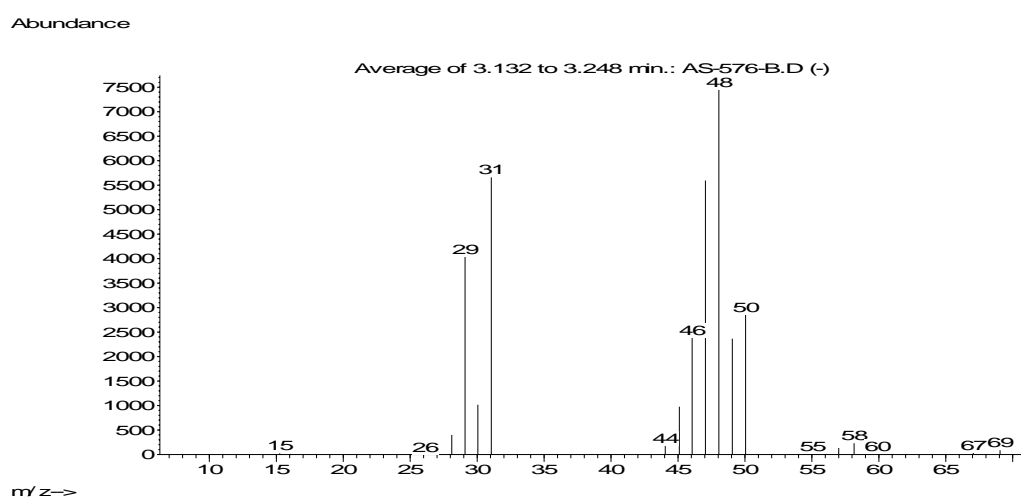
Supplementary Figure 15. Mass spectra of compounds found in the reaction mixture.



Supplementary Figure 16. Mass spectra of methanol (a) and formic acid (b) obtained in course of oxidation of CH_4 (53 %) and $^{13}\text{CH}_4$ (47 %).

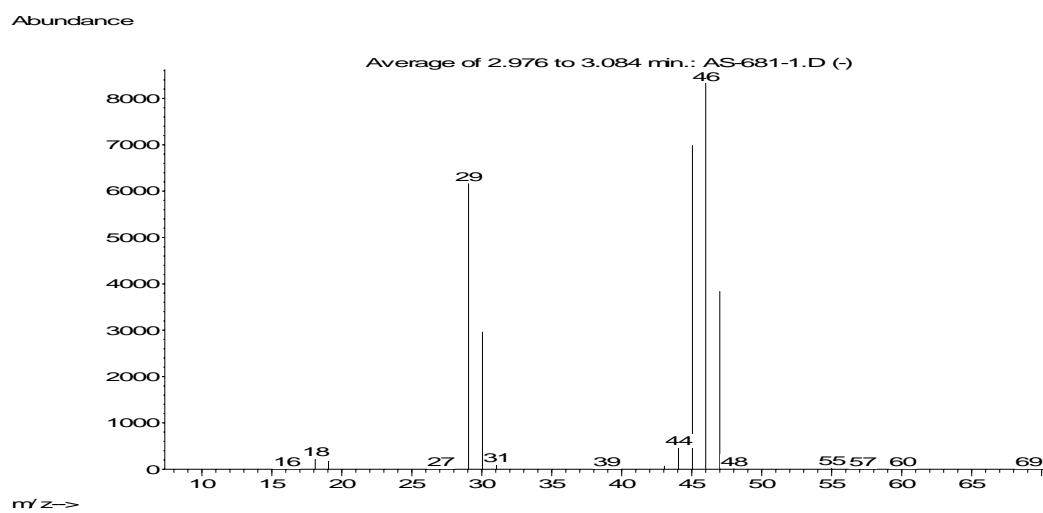


a



b

Supplementary Figure 17. Mass spectra of methanol (a) and formic acid (b) obtained in course of oxidation of methane by $\text{H}_2^{16}\text{O}_2$ in H_2^{18}O .



Supplementary Figure 18. Mass spectrum of formic acid obtained in course of oxidation of methane by $\text{H}_2^{16}\text{O}_2$ in CD_3CN .